Kinematics of slab tear faults during subduction segmentation and implications for Italian magmatism

Gideon Rosenbaum,[1] Massimo Gasparon,[1] Francesco P. Lucente,[2] Angelo Peccerillo,[3] and Meghan S. Miller[4]

Received 21 April 2007; revised 24 October 2007; accepted 4 February 2008; published 25 April 2008.

[1] Tectonic activity in convergent plate boundaries commonly involves backward migration (rollback) of narrow subducting slabs and segmentation of subduction zones through slab tearing. Here we investigate this process in the Italian region by integrating seismic tomography data with spatiotemporal analysis of magmatic rocks and kinematic reconstructions. Seismic tomography results show gaps within the subducting lithosphere, which are interpreted as deep (100–500 km) subvertical tear faults. The development of such tear faults is consistent with proposed kinematic reconstructions, in which different rates of subduction rollback affected different parts of the subduction zone. We further suggest a possible link between the development of tear faults and the occurrence of regional magmatic activity with transitional geochemical signatures between arc type and OIB type, associated with slab tearing and slab breakoff. We conclude that lithospheric-scale tear faults play a fundamental role in the destruction of subduction zones. As such, they should be incorporated into reconstructions of ancient convergent margins, where tear faults are possibly represented by continental lineaments linked with magmatism and mineralization. **Citation:** Rosenbaum, G., M. Gasparon, F. P. Lucente, A. Peccerillo, and M. S. Miller (2008), Kinematics of slab tear faults during subduction segmentation and implications for Italian magmatism, *Tectonics*, *27*, TC2008, doi:10.1029/2007TC002143.

1. Introduction

[2] Tearing and subsequent breakoff of subducting lithospheric slabs is a process well documented by geophysical observations [e.g., *Chatelain et al.*, 1992; *Carminati et al.*, 1998; *Wortel and Spakman*, 2000; *Lallemand et al.*, 2001; *Levin et al.*, 2002; *Miller et al.*, 2006]. Slab tearing is typically triggered by local collisional events [*Sacks and Secor*, 1990] combined with variations in the velocity of subduction rollback along the length of the subduction system [*Govers and Wortel*, 2005]. The process of slab tearing creates gaps in the lithosphere that localize asthenospheric upwelling, thus triggering magmatic activity that could potentially deviate from the geochemistry of typical subduction-related magmas [*von Blanckenburg and Davies*, 1995; *Maury et al.*, 2000; *Guivel et al.*, 2006].

[3] Slab tearing plays a major role in the development of segmented subduction zones [*Woodcock and Daly*, 1986], particularly during subduction rollback of narrow slab segments [*Govers and Wortel*, 2005; *Schellart et al.*, 2007]. Slab tear faults are likely to link two adjacent segments of the subduction zone and to accommodate horizontal movements if different rollback velocities operate in the two segments (Figures 1d and 1e). *Govers and Wortel* [2005] have identified the existence of such faults in the North Fiji Basin (Hunter fracture zone [*Schellart et al.*, 2002]), on the island of Sulawesi (Palu fault), and at the edges of the Calabrian, Caribbean and Scotia arcs.

[4] In this paper, we investigate the geometry and kinematics of slab tear faults in Italy (Figure 2), with the aim of developing a unifying geodynamic model for the region. This area is one of the world's best examples of a collisional belt in which the earlier history of subduction rollback and slab segmentation is relatively well preserved [*Malinverno and Ryan*, 1986; *Doglioni et al.*, 1999]. During the last 10 Ma, convergence between Africa and stable Europe was relatively slow [*Dewey et al.*, 1989; *Rosenbaum et al.*, 2002; *Hollenstein et al.*, 2003], and lateral movements along the plate boundary were predominantly governed by subduction rollback [*Malinverno and Ryan*, 1986; *Royden et al.*, 1987; *Patacca and Scandone*, 1989; *Faccenna et al.*, 2001; *Rosenbaum and Lister*, 2004]. Rollback velocities varied along the strike of the subduction zone, a process that involved tearing and segmentation of the subducting lithospheric slab [*Royden et al.*, 1987; *Doglioni et al.*, 1994].

[5] Seismic tomography data indicate that the subducting lithospheric slab beneath Italy is not continuous, and that a prominent slab window exists beneath the central Apennines [*Lucente et al.*, 1999; *Wortel and Spakman*, 2000; *Piromallo and Morelli*, 2003]. The crustal response to the development of this slab window has been shown to be associated with lateral changes in the architecture of foredeep basins [*van der Meulen et al.*, 1998], rapid uplift [*van der Meulen et al.*, 2000], and possible tear-related magmatism [*Marani and Trua*, 2002; *Faccenna et al.*, 2005; *De Astis et al.*, 2006]. However, the geometry of associated tear faults, and their role during the development of the central Apennine slab window are not clear. These issues

[1]School of Physical Sciences, University of Queensland, Brisbane, Queensland, Australia.
[2]Istituto Nazionale di Geofisica e Vulcanologia, CNT, Rome, Italy.
[3]Dipartimento di Scienze della Terra, Università degli Studi di Perugia, Perugia, Italy.
[4]Department of Earth Science, Rice University, Houston, Texas, USA.

0278-7407/08/2007TC002143

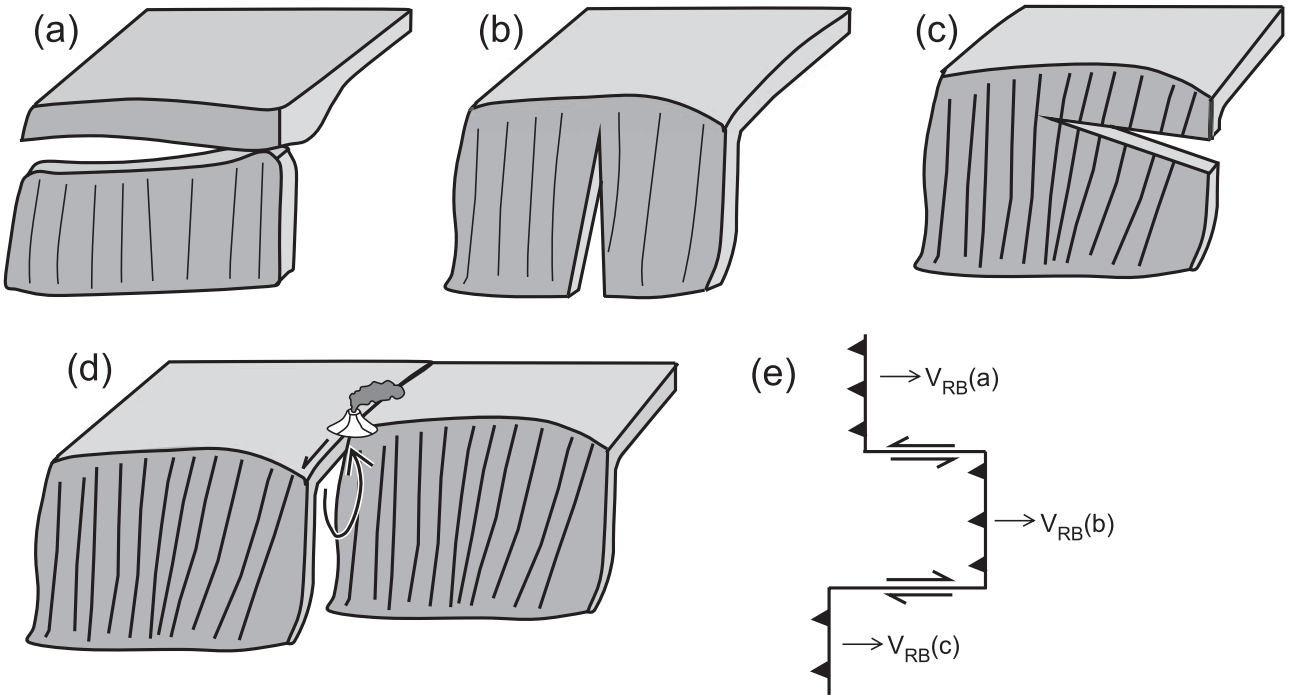

Figure 1. Schematic illustrations of processes involving tearing and/or breakoff of subducting slabs. (a) Slab breakoff associated with the final detachment of a lithospheric slab. Slab breakoff commonly follows collisional processes and is sometime referred as collisional delamination. (b) A vertical propagating tear. (c) A horizontal propagating tear. (d) Three-dimensional structure of a lithospheric tear fault that separates two subducting segments. The curved arrow indicates upwelling of hot asthenospheric material, which can trigger tear-related magmatism during fault propagation. (e) Two tear faults (indicated by double arrows) that connect three segments of a subduction system characterized by differential rollback velocities ($V_{RB}(b) > V_{RB}(a) > V_{RB}(c)$). Triangles indicate the direction of subduction and single arrows indicate the direction of subduction rollback.

are addressed here by coupling kinematic reconstructions [*Rosenbaum and Lister*, 2004] with the geometry of relatively cold lithospheric slab segments as deduced from seismic tomography data [*Lucente et al.*, 1999]. This approach enables us to reconstruct the development and propagation of slab tear faults during the process of subduction rollback, and to better understand the distribution of Plio-Quaternary magmatism in Italy in the context of the regional geodynamics.

2. Terminology

[6] The terms delamination, slab detachment, slab tearing and slab breakoff are interchangeably used in the literature to describe a number of slightly different tectonic processes. Delamination is the process, in which cooler and denser lithospheric mantle is peeled away from the overlying continental crust and sinks vertically into the underlying asthenosphere [*Bird*, 1978, 1979]. This concept has predominantly been applied to describe the foundering of overthickened lithospheric roots in orogenic belts [*Houseman et al.*, 1981; *Platt and England*, 1994]. While delamination is not restricted to subduction processes, rupturing and sinking of a subducting lithosphere is commonly termed slab breakoff (Figure 1a) [*Davies and von Blanckenburg*, 1995; *von Blanckenburg and Davies*, 1995; *Cloos et al.*, 2005]. The term slab detachment is sometime used as a synonym to slab breakoff [*Levin et al.*, 2002; *Gerya et al.*, 2004], but more commonly as the process leading to slab breakoff, involving a lateral propagation of a horizontal tear [e.g., *van der Meulen et al.*, 1998, 2000; *Wortel and Spakman*, 2000; *Faccenna et al.*, 2006; *Martin*, 2006].

[7] Slab tearing is commonly used in the literature to describe a propagating tear in the slab. Such tears can be either vertical (Figure 1b) or horizontal (Figure 1c). The process of slab tearing as described in this paper is associated with vertical tears that laterally propagating along slab tear faults (Figures 1d and 1e). Such structures are similar to those termed by *Govers and Wortel* [2005] as Subduction-Transform Edge Propagator (STEP) faults.

3. Seismic Tomography

[8] The upper mantle velocity structure beneath Italy and the Tyrrhenian Sea is now well established, and all recent tomographic models of the area are consistent in the gross features [*Lucente et al.*, 1999; *Wortel and Spakman*, 2000; *Piromallo and Morelli*, 2003]. The two most prominent

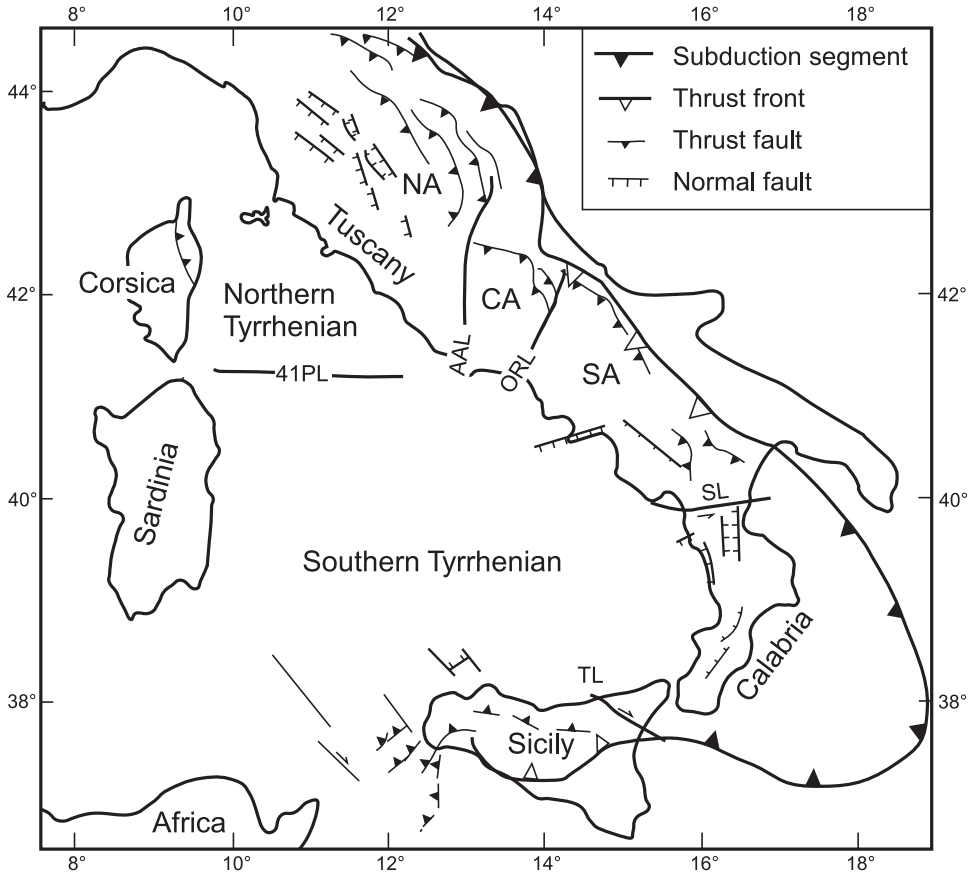

Figure 2. Structural setting of the Tyrrhenian Sea and the Apennine belt [after *Rosenbaum and Lister*, 2004, and references therein]. Filled triangles, subduction segments; open triangles, thrust fronts; 41PL, 41°N parallel line; AAL, Anzio-Ancona Line; CA, Central Apennines; NA, Northern Apennines; ORL, Ortona-Roccamonfina Line; SA, Southern Apennines; SL, Sangineto line; TL, Taormina line.

features are (1) a narrow lithospheric slab segment (the Ionian slab) subducting steeply beneath Calabria down to a depth of 670 km and becoming horizontal parallel to the 670 km discontinuity (where it fails to penetrate the lower mantle); and (2) a remnant slab segment (the Adriatic slab) subducting subvertically beneath the northern Apennines. The absence of high-velocity perturbation between these two slab segments (in the central and southern Apennines) is interpreted to represent the earlier cessation of subduction in this area [*Lucente and Speranza*, 2001]. At depth of >250 km, the northern Apennine and Ionian slabs possibly join into a single fast anomaly (Figure 3).

[9] The tomographic images (Figures 3–5) are based on the distribution of P wave positive velocity anomalies [*Lucente et al.*, 1999]. The 3-D morphology of subducting lithospheric slab beneath Italy (Figure 3), based on an enveloping surface defined by the 1.5% positive anomaly contour, shows a strongly segmented complex structure. The actual tears of the lithospheric slab are recognized in zones of negative velocity anomalies in cross sections that run parallel to the strike of the subduction zone (Figure 4). A more detailed mapping of the geometry of such tears is done by projecting only positive (> 1%) velocity anomalies down to a depth of 670 km (Figure 5).

[10] Owing to the use of high-quality data, our tomographic model suffers from relatively low regularization, which potentially allows a more accurate representation of both the amplitude of the velocity anomalies, and of their spatial distribution (i.e., thickness and lateral continuity) at depths of >50 km [*Lucente et al.*, 1999]. In order to assess this accuracy, we conducted detailed resolution analyses by computing sensitivity tests [e.g., *van der Hilst et al.*, 1993; *Piromallo and Morelli*, 2003], which address the resolution of the inversion scheme in terms of its ability to retrieve a known input model, given the ray coverage used in the real data inversion. Such sensitivity analyses provide comprehensive visual inspection of the model's spatial resolution, showing a measure of the wavelength of the structures that can be judged as reliable in various portions of the model. The performed synthetic tests are presented in Appendix A and in the auxiliary material Figures S1–S4[1].

[11] Results of the sensitivity analysis confirm that nonperipheral areas of the model (i.e., where the diagonal elements of the resolution matrix are higher than 0.6 [cf. *Lucente et al.*, 1999] suffer from very little smearing of the

[1]Auxiliary materials are available in the HTML. doi:10.1029/2007TC002143.

anomalies. Structures are well resolved down to wavelength comparable with the block dimensions in each layer (varying from 52.5 to 95 km with increasing depth). Identified discontinuities and tear faults (Figure 5) are located in the well resolved nonperipheral areas, and are therefore regarded as reliable structures within the resolution power of the inversion method (see Figure A1 and auxiliary material Figures S1–S4). This, in turn, enables us to incorporate the present-day 3-D geometry in a kinematic reconstruction, emphasizing the role of subduction rollback and propagating tear faults.

4. Slab Tear Faults in the Italian Region

4.1. Distribution of Slab Tear Faults as Inferred From Seismic Tomography

[12] A major feature recognized in the tomographic images (Figures 4 and 5) is the complex geometry of lithospheric slab segments that are possibly separated by slab tear faults. The existence of a slab window down to depths of >200 km is recognized in the central Apennines (section A-A′ in Figure 4). This asthenospheric window is bounded by two tear faults, as mapped in Figure 5. Cross section A-A′ also shows a weak expression of the two southern Apennine tear faults, associated with a zone of lower seismic velocities down to depths of 250 km around latitude 40.5°. In a section parallel to Sicily (section B-B′ in Figure 4), three negative seismic anomalies down to depths of 100–200 km delineate the boundaries of a strongly segmented lithospheric structure. In the northern Tyrrhenian (section C-C′ in Figure 4) possible tear faults bound a low-velocity zone between latitudes 42° and 43°.

[13] The complex lithospheric structure revealed in Figures 4 and 5 is construed to represent distinct slab segments separated by relatively linear seismic velocity discontinuities. We interpret these lines as lithospheric tear faults, which accommodated strike-slip displacements during slab tearing propagation. The seismic tomography model enables us to estimate the depth of these tear faults on the basis of the depth of the displaced slab-related anomalies. The crustal expression of such faults is possibly related to the existence of orogen perpendicular strike-slip faults within the Apennine fold-and-thrust belt [e.g., *Di Luccio et al.*, 2005; *Billi et al.*, 2006; *Scrocca*, 2006]. Some of these structures show relatively deep seismicity (~20 km [*Di Luccio et al.*, 2005]), indicating that they are deep rooted structures (as opposed to thin-skinned accommodation faults).

[14] The deepest recognized tear fault (down to a depth of 550 km) runs E-W parallel to latitude 42°N (42°10′ ± 10′) (Figure 5). It is indicated by the transition from positive seismic velocities north of the fault to an area that generally lacks positive anomalies (with the exception of a single displaced slab segment around longitude 11–12°E). This tear fault continues at slightly shallower depths (< 340 km) and meets one of the major structural boundary, the so-called Ancona-Anzio line (Figure 2) that crosses the Apennines from north to south and separates the northern Apennine belt (Umbria-Marche arc) from the central Apennines. Another deep (< 440 km) lithospheric tear fault, defined by the southern extension of the displaced slab segment around longitude 11–12°E, runs parallel to latitude 41°N (Figure 5). This lithospheric-scale fault is a well known structure (41°N parallel line), which separates a domain with relatively low crustal extension in the northern Tyrrhenian, from an area that underwent much higher degree of crustal extension, leading to the formation of oceanic crust in the southern Tyrrhenian Sea [*Sartori*, 1990]. The crustal discontinuity parallel to latitude 41°N was also recognized in seismic profiles and was shown to be associated with a magnetic and free-air gravity anomaly [*Spadini and Wezel*, 1994; *Bruno et al.*, 2000].

[15] Similarly to the 42°N fault further north, the tear fault associated with the 41°N parallel line changes its orientation in the Apennines to almost N-S. It is recognized at depth of <250 km, dividing the two domains of the Roman Province and the Ernici-Roccamonfina volcanoes, which have different petrologic and geochemical signatures [*Peccerillo and Panza*, 1999; *Frezzotti et al.*, 2007]. The possible surface expression of this fault is the Ortona-Roccamonfina Line (Figure 2).

[16] Slab tear faults along the margin of the southern Tyrrhenian Sea operated at depths of 100–340 km, and are characterized by NE-SW faults in the southern Apennines, and NW-SE faults in Sicily (see also cross section B-B′ in Figure 4). The existence of such lithospheric-scale tear faults, in particular those rooting the left lateral Sangineto line and the right lateral Taormina line (Figure 2), has been suggested by previous authors [*Govers and Wortel*, 2005; *Panza et al.*, 2007]. Conversely, other authors interpreted the Taormina line as the edge of the thin-skinned Calabrian nappes [*Lentini et al.*, 1994]. On the basis of the deep structure revealed by seismic tomography, we think that the arrangement of conjugate faults represents lithospheric-scale strain accommodation during the eastward rollback of the Ionian subduction zone. The deep structures roughly mimic crustal structures, which show similar orientations of conjugate strike-slip faults and opposite senses of block rotations around vertical axes [*Van Dijk and Scheepers*, 1995; *Speranza et al.*, 1999; *Renda et al.*, 2000; *Mattei et al.*, 2004]. The surface expression of the NW-SE right lateral faults in NE Sicily is particularly well documented [*Billi et al.*, 2006], and possibly involves active seismicity [*Goes et al.*, 2004].

4.2. Development and Propagation of Slab Tear Faults

[17] The kinematic evolution of slab tear faults is schematically illustrated in Figure 6. The reconstruction is based on the detailed spatiotemporal analysis of *Rosenbaum and Lister* [2004], where an extensive amount of geological data have been used to constrain the kinematic evolution of the Tyrrhenian Sea and the Apennine belt. These data include the migration of shortening and extensional structures, the first appearance of syn-rift sediments, the distribution of palaeogeographic domains, the rotation of crustal blocks as inferred from palaeomagnetic data, and the spatiotemporal distribution of magmatic rocks [*Rosenbaum and Lister*, 2004]. The reconstruction also shows the possible location

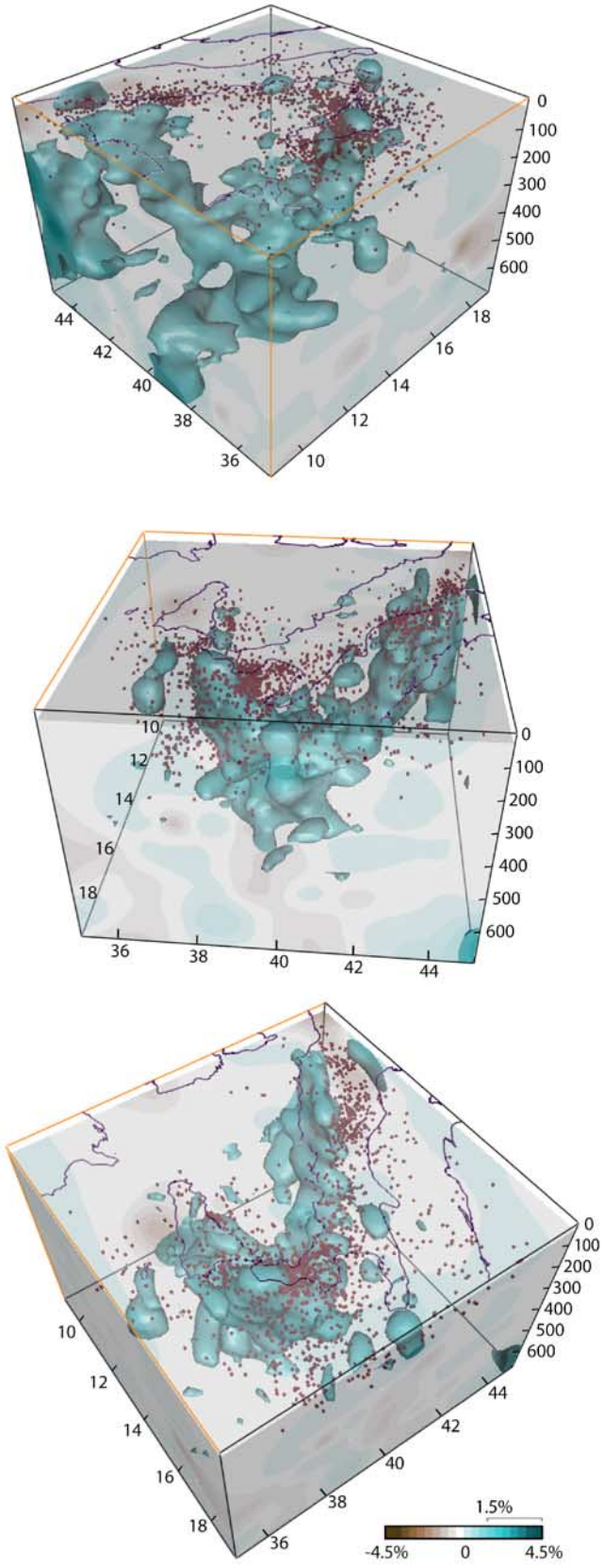

of lithospheric slab segments as projected from the present-day position at depths of 100–170 km (see Figure 5).

5. Magmatism in the Italian Region

5.1. Spatiotemporal Distribution

[18] An important outcome of the kinematic reconstruction is the apparent link between the propagating tear faults and the spatial and temporal distribution of magmatism (Figure 6 and Table 1). Magmatism in Italy is manifested by a large spectrum of magmas ranging from subduction-related calc-alkaline and ultra-potassic magmas to intraplate oceanic island basalts (OIB), and Mid Oceanic Ridge Basalts (MORB) (Figure 7) [*Peccerillo*, 2005]. Here we show that the geochemical affinities of these magmas are generally consistent with our geodynamic model, thus further supporting the suggestion that the Apennine subduction zone was subjected to segmentation through slab tear faulting. Our model, however, does not attempt to explain all the complex features of the petrology of the volcanic edifices [e.g., *Peccerillo*, 2001, 2005; *Gasperini et al.*, 2002; *Panza et al.*, 2007].

[19] The early stage of magmatic activity in the Tyrrhenian Sea, which followed abundant calc-alkaline magmatism in Sardinia, was associated with 9–6 Ma intrusive and extrusive magmatism in Capraia, Elba, Montecristo and Vercelli seamount (Figures 6a and 6b). Magmatism appears immediately above the Miocene subducting slab and is attributed to the subduction-related magmatic arc. By ~5 Ma, this magmatic arc has migrated eastward [*Civetta et al.*, 1978] from Capraia, Vercelli Seamount, Montecristo, and western Elba to eastern Elba and Giglio islands (Figure 6c). In the southern Tyrrhenian, direct evidence for subduction-related magmas is less clear, but there have been suggestions for the existence of a submerged Pliocene subduction-related volcanic arc [*Sartori*, 1986, 2005]. The location of this arc [see *Sartori*, 1986, Figure 3] exactly corresponds to the geometry of the subduction zone at 6–4 Ma, as shown in Figure 6c.

[20] Simultaneously with the production of Pliocene subduction-related magmas, further magmatism was generated by decompressional melting of asthenospheric mantle in extensional regions and gaps in the slab corresponding to tear faults. One of these tear faults propagated from the northern tip of Corsica to southern Tuscany, producing, at ~4.8 Ma, mantle-derived shoshonites in Capraia that are characterized by lower ratios of Large Ion Lithophile Elements versus High Field Strength Elements (LILE/HFSE) compared with the older activity (see section 5.2). Further east, the crustal uplift in southern Tuscany and the production of anatectic felsic magmas (San Vincenzo,

Figure 3. Interpreted 3-D morphology of subducting lithospheric segments beneath Italy based on seismic tomography [*Lucente et al.*, 1999]. The enveloping surface represents the 1.5% positive anomaly contour. Brown dots indicate the instrumental seismicity recorded in the period 1981–2002 by the Italian Permanent Seismic Network (RSNC) [*Castello et al.*, 2004].

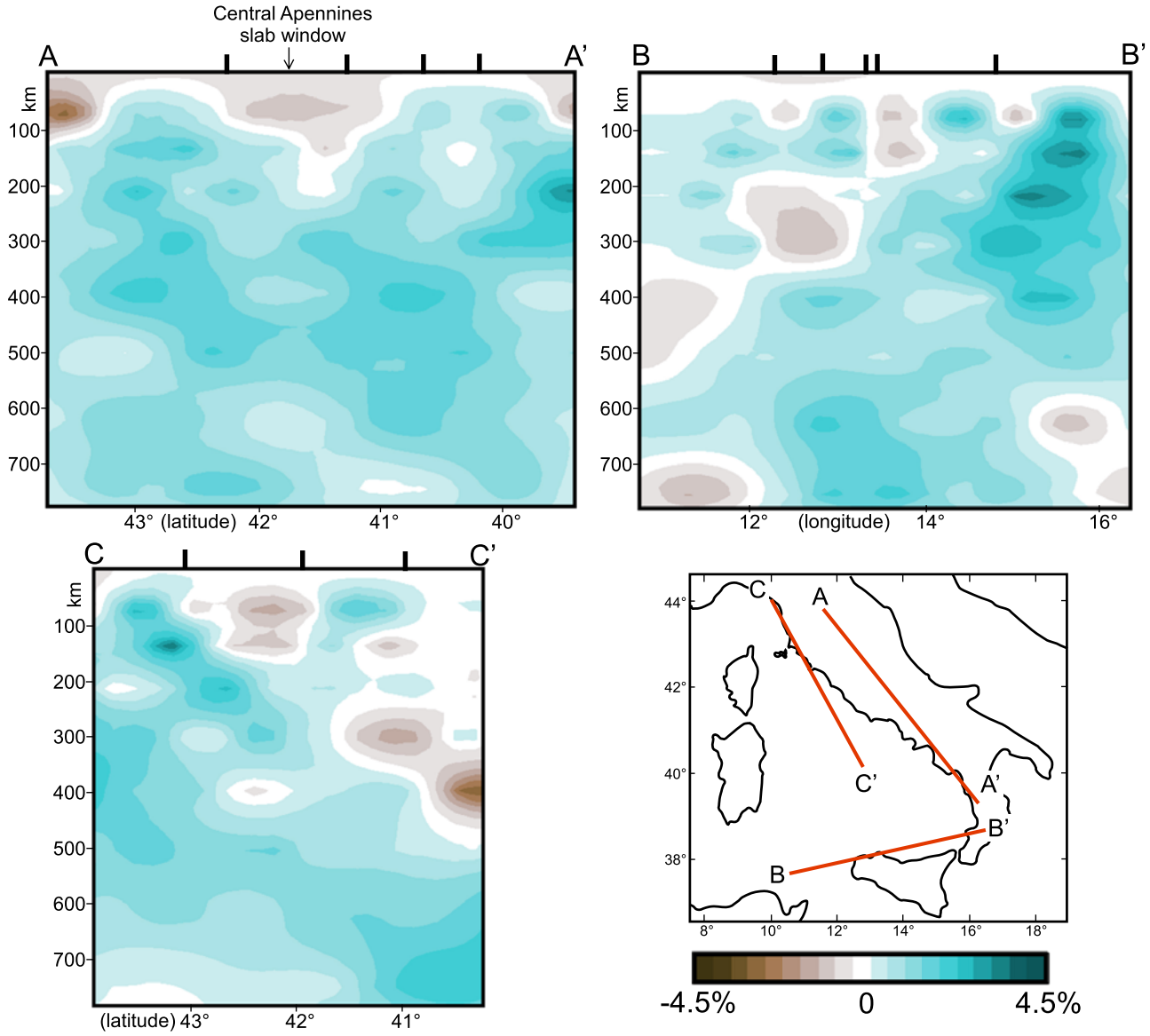

Figure 4. Tomographic cross sections highlighting orogen-perpendicular lithospheric-scale structures. Locations of slab tear faults as mapped in Figure 5 are indicated by short black lines. A detailed analysis of the resolution power of the inversion method along these cross sections is shown in the auxiliary material Figure S4.

Castel di Pietra and Gavorrano) along the same fault (Figure 6c) are also interpreted to result from the combination of slab tearing and arc magmatism. Contemporaneous volcanism located along tear faults also occurred further south in Anchise Seamount and Ponza Island. The latter was subjected to magmatism from 4.2 to 1 Ma [*Cadoux et al.*, 2005], and is considered as the northern end of the southern Tyrrhenian Pliocene arc [*Sartori*, 1986], which was transected by the tear fault of the 41°N parallel line.

[21] The distribution of some of the younger (4–2 Ma) magmatic activity was also focused along the deeper tear faults (Figure 6d). This includes a cluster of subduction/tear-related magmatic centers (Tolfa, Manziana and Cerite) in the area where the deep tear fault parallel to latitude 42°N intersected with the Italian peninsula. In the south, the occurrence of magmatism in Volturno (>2 Ma) and Ponza (4.2 to 1 Ma) also coincide with slab tearing. Subsequently, during the last 2 Ma (Figure 6e), the central Apennines were subjected to widespread tear-related magmatic activity and magmatism induced by breakoff of the lithospheric slab [*De Astis et al.*, 2006; *Panza et al.*, 2007]. We interpret this magmatic phase as the geodynamic expression for the formation of the central Apennine asthenospheric window following slab segmentation, and the local destruction of the subduction system. Further south, arc magmatism in the Aeolian Islands has been generated by subduction of the narrow Ionian slab, whereas the combination of rapid slab rollback and slab tearing resulted in asthenospheric upwell-

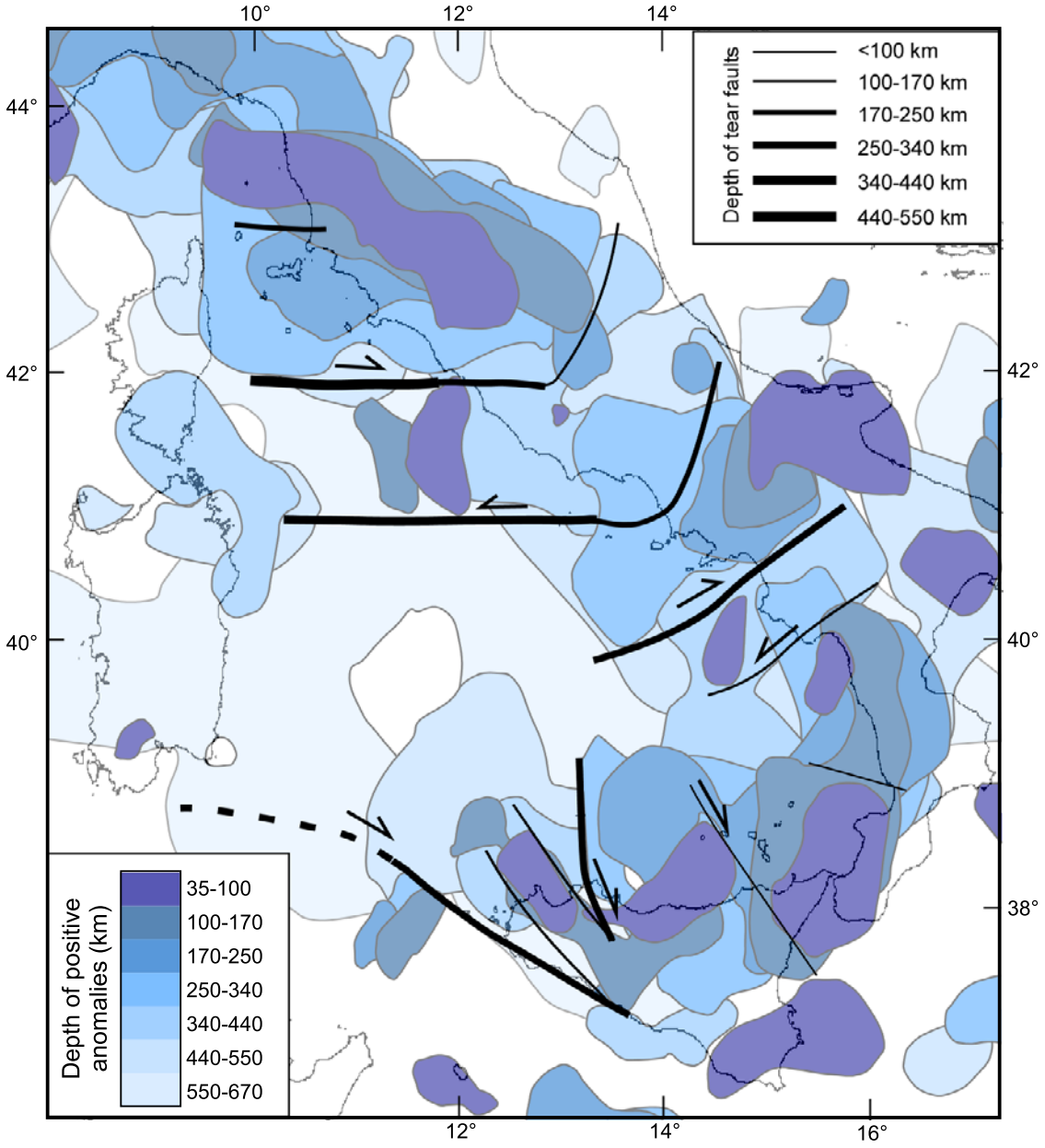

Figure 5. Upper mantle structure in Italy and the Tyrrhenian Sea based on positive P wave seismic anomalies [*Lucente et al.*, 1999]. The shaded areas indicate positive anomalies at different lithospheric depth ranges. They are interpreted to represent remnant subducting slabs, separated from each other by lithospheric-scale tear faults (black lines).

ing at Mt Etna [*Gvirtzman and Nur*, 1999; *Doglioni et al.*, 2001; *Schiano et al.*, 2001].

5.2. Geochemical Evidence

[22] The link between the regional geodynamics and geochemical evidence on the depth of melting and extent of mantle metasomatism is not straightforward. Compositional variations and mantle heterogeneity can be modified by rollback-related horizontal mantle flow [*Funiciello et al.*, 2003; *Kincaid and Griffiths*, 2003; *Schellart*, 2004] and are affected by variable types and intensities of metasomatism [*Panza et al.*, 2007]. However, whereas some element abundances and ratios (e.g., LILE/HFSE) and isotopic signatures depend on nature and intensity of metasomatism, other compositional features, such as HFSE ratios do not depend so much on metasomatism but reflect premetasomatic mantle sources. Some major element ratios (e.g., Ca/Al of primary melts, which have not suffered clinopyroxene and/or plagioclase fractionation) depend on source mineralogy. The combination of all these features provides a further support for the geodynamic reconstruction (Figure 6).

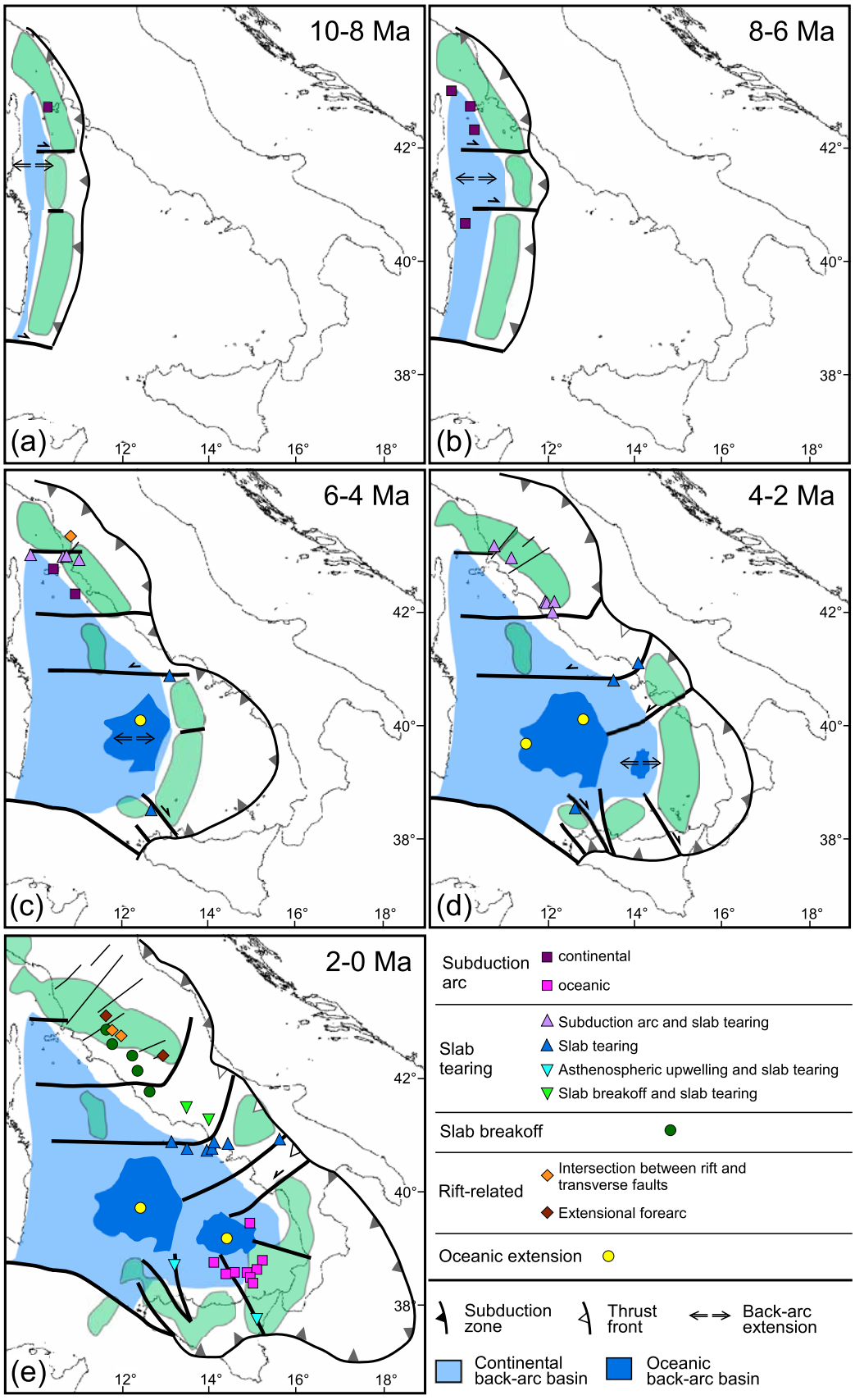
10-8 Ma
8-6 Ma
6-4 Ma
4-2 Ma
2-0 Ma
(a)
(b)
(c)
(d)
(e)
42°
40°
38°
12°
14°
16°
18°
Subduction arc
continental
oceanic
Slab tearing
Subduction arc and slab tearing
Slab tearing
Asthenospheric upwelling and slab tearing
Slab breakoff and slab tearing
Slab breakoff
Rift-related
Intersection between rift and transverse faults
Extensional forearc
Oceanic extension
Subduction zone
Thrust front
Back-arc extension
Continental back-arc basin
Oceanic back-arc basin

Figure 6

Table 1. Magmatic Centers in the Italian Region and Corresponding Geochronological Ages[a]

Number	Name	Age, Ma
1	Montecatini Val di Cecina and Orciatico	4.1
2	Monteverdi	3.8
3	Capraia	7.5–7.1 & 4.8
4	Campiglia	5.0
5	San Vincenzo	4.7–4.4
6	San Venanzo	0.26
7	Roccastrada	2.5–2.2
8	Castel di Pietra and Gavorrano	4.4–4.3
9	Amiata	0.3–0.2
10	Radicofani	1.3
11	Torre Alfina	0.8
12	Mt. Capanne, Elba	8.5–6.2
13	Porto Azzurro, Elba	5.8–5.1
14	Vulsini	0.6–0.1
15	Cimini	1.3–0.9
16	Montecristo	7.1
17	Giglio	5.1
18	Cupaello	0.64
19	Tolfa	3.8–2.3
20	Manziana	3.6
21	Cerite	2.4
22	Vico and Sabatini	0.8–0.1
23	Alban Hills	0.6–0.04
24	Ernici	0.7–0.08
25	Roccamonfina	0.6–0.1
26	Volturno	>2
27	Ponza	4.2–3.0 & 1.0
28	Ventotene	0.8–<0.2
29	Phlegrean Fields	0.2–0
30	Procida	0.06–0.02
31	Ischia	0.15–0
32	Vesuvius	0.03–0
33	Vulture	0.8–0.13
34	Vercelli seamount	7.5–6.5
35	ODP 655	4.6–4.0
36	ODP 651	3.0–2.6
37	Magnaghi seamount	3.0–2.7
38	Vavilov seamount	0.4–<0.1
39	ODP 650	1.9–1.6
40	Palinuro seamount	0.8–0.3
41	Marsili seamount	0.8–0
42	Anchise seamount	5.3–3.5
43	Ustica	0.75–0.13
44	Enarete and Eolo seamounts	0.8–0.6
45	Alicudi	0.06–0.03
46	Filicudi	1.02 & 0.4–0.04
47	Stromboli	0.2–0
48	Panarea	0.8–0.01
49	Salina	0.4–0.01
50	Lipari	<0.25
51	Vulcano	<0.12
52	Etna	0.5–0

[a]See Figure 7 for location of magmatic centers. For references see auxiliary material Table S1.

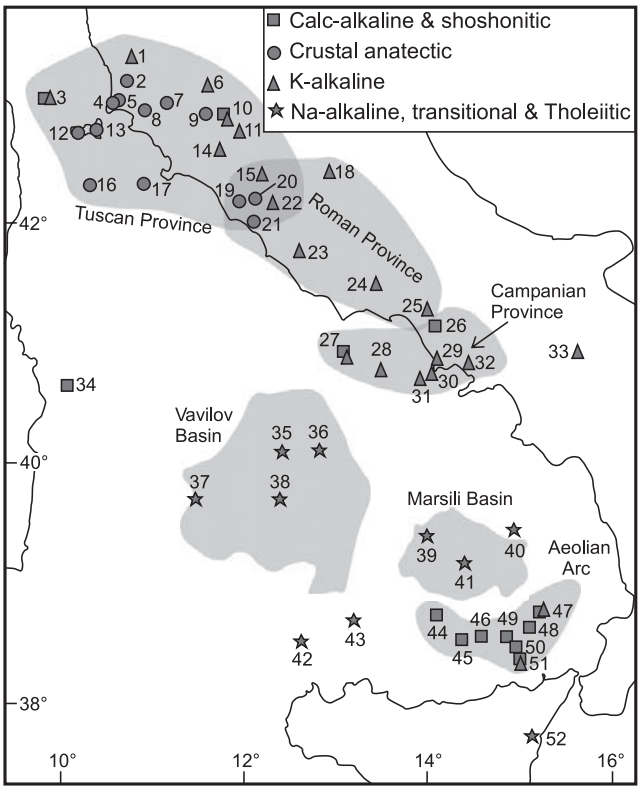

Figure 7. Spatial distribution and petrochemical affinity of young (< 10 Ma) magmatic centers in the Italian peninsula, Sicily and the Tyrrhenian Sea [after *Peccerillo*, 2005]. OIB-type magmatic centers in the African foreland (e.g., Hyblean Mountains, Pantelerria, Linosa) and in Sardinia are not included. Numbers correspond to the list in Table 1.

[23] Most significant geochemical evidence includes elemental LILE/HFSE ratios, such as La/Nb and radiogenic isotopes (e.g., $^{87}Sr/^{86}Sr$). In Figure 8 we use La/Nb and $^{87}Sr/^{86}Sr$ values to identify different degrees of mantle metasomatism. Low La/Nb and $^{87}Sr/^{86}Sr$ values in mafic magmas indicate mantle source, probably asthenosphere, which suffered lesser degree of subduction-related mantle metasomatism. OIB-type magmas typically have low La/Nb. Strongly fractionated and anatectic melts have relatively low (but highly variable) La/Nb and high $^{87}Sr/^{86}Sr$ values, while magmas derived from a subduction-metasomatized mantle are characterized by high La/Nb and variable $^{87}Sr/^{86}Sr$ values.

[24] Continental arc-related magmatism in central Italy is characterized by moderately elevated $^{87}Sr/^{86}Sr$ values (around 0.708–0.709), LREE/HREE values (La/Yb $\sim$ 20–30) and LILE/HFSE values (La/Nb > 2 in mafic-intermediate rocks;

Figure 6. Reconstruction of the kinematic evolution of the Tyrrhenian Sea and the Apennine belt. The reconstruction shows the development and propagation of slab tear faults during the segmentation of the retreating subduction zone. The reconstruction images are snapshots at the minimum age of each time interval and show the accumulated magmatic activity during each interval (see Figure 7). The thin lines in the northern Apennines indicate the location of crustal transfer faults [after *Decandia et al.*, 2001]. The classification of magmas based on their geodynamic context is supported by geochemical evidence (see section 5.2 in the text and Figure 8).

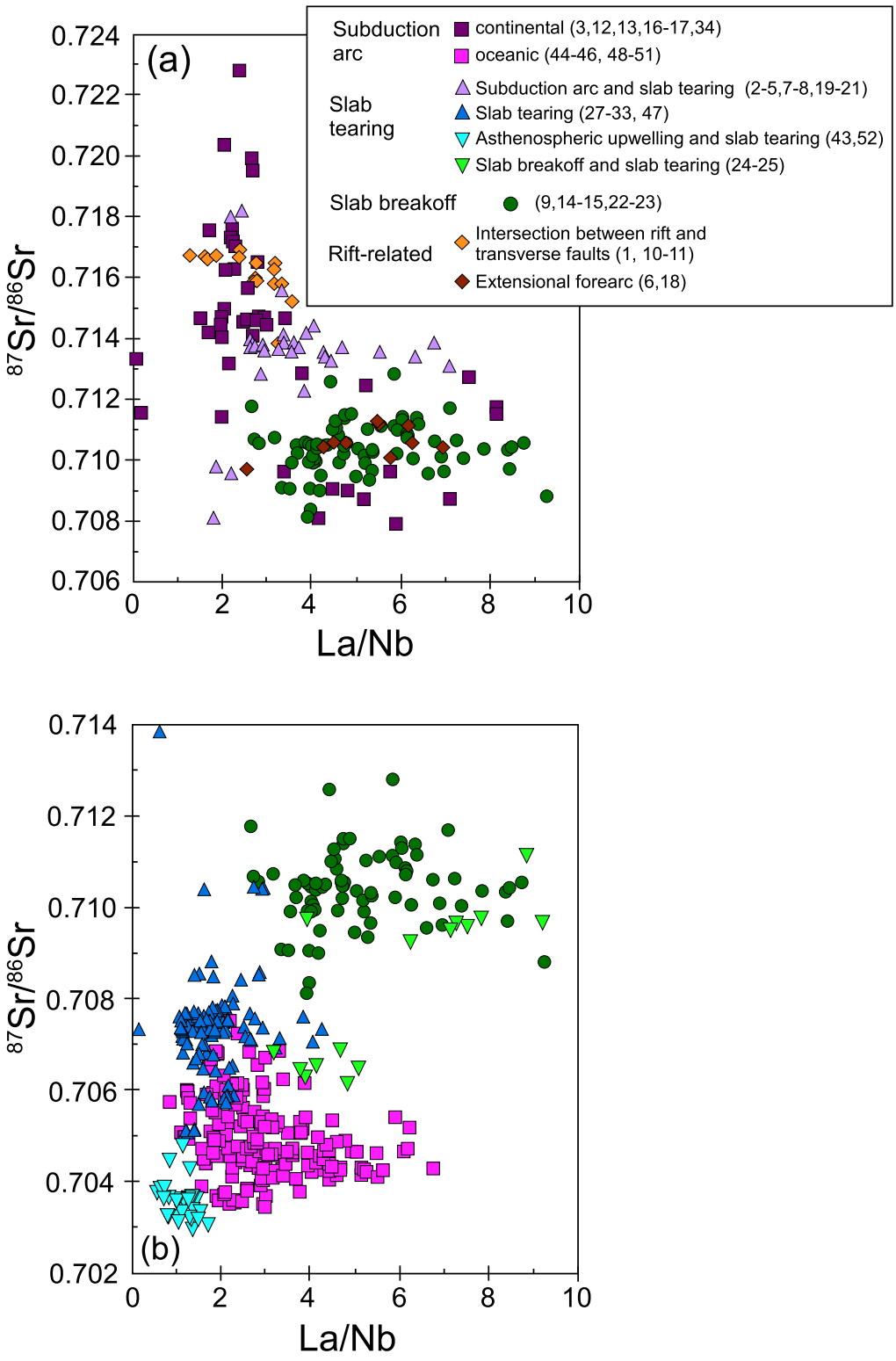

Figure 8. La/Nb versus $^{87}Sr/^{86}Sr$ values for the young (< 10 Ma) Italian magmatic rocks listed in auxiliary material Table S1 and Figure 7. Data are classified on the basis of the geodynamic context as shown in Figure 6, and are presented in two diagrams to enhance readability. Numbers refer to localities in Figure 7. (a) Data from the Tuscan magmatic province and rift-related magmatism. (b) Data from the southern Tyrrhenian and central-southern Italy. The Roman magmatic province is shown in both figures for reference. All data are taken from the compilation of *Peccerillo* [2005].

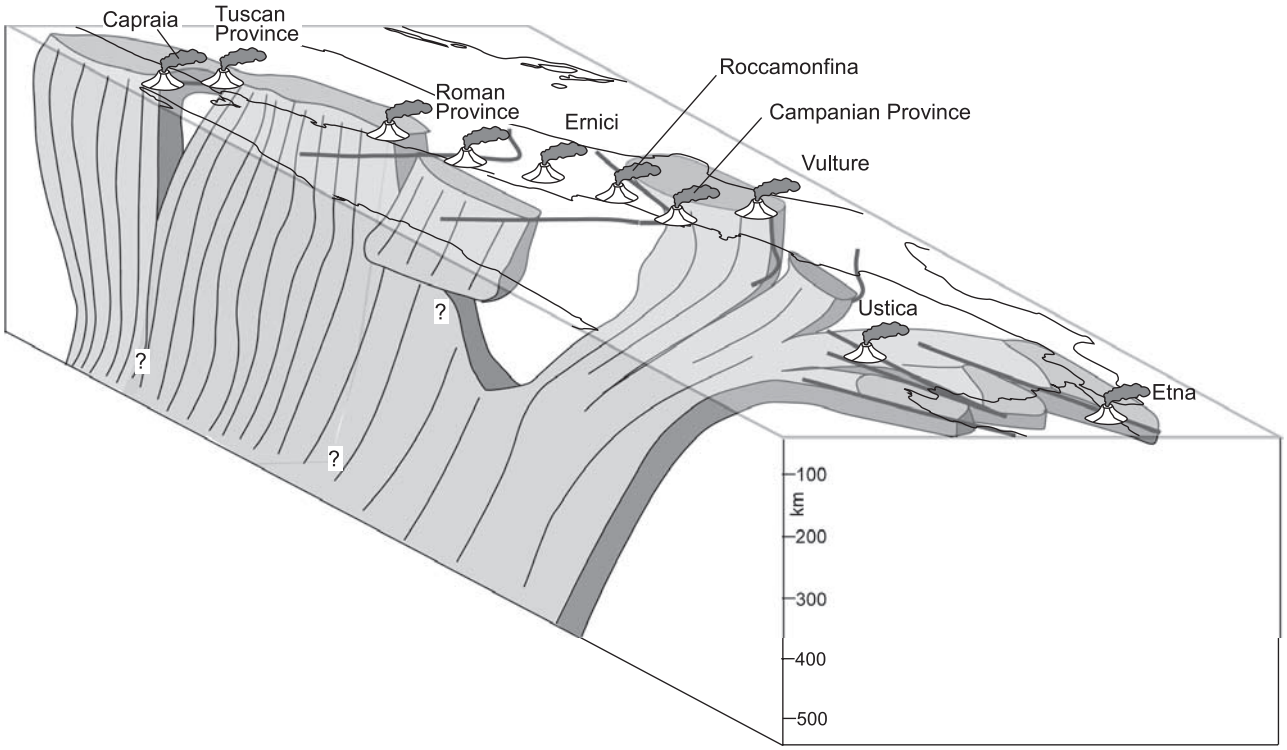

Figure 9. Simplified 3-D sketch of the subducting lithosphere beneath Italy showing the approximate spatial distribution of tear faults and the geometry of the central Apennine slab window. Selected tear-related and slab breakoff-related magmatic centers are also shown.

Figure 8a). In contrast, $^{143}Nd/^{144}Nd$ values are relatively low. We find these ratios in 7.5 Ma old intermediate calc-alkaline volcanic rocks at Capraia, mafic inclusions in granites (Elba), and predominantly granitic-anatectic rocks (Elba, Montecristo, Giglio, Vercelli Seamount) derived from the mixing of calc-alkaline melts with crustal anatectic magmas. Some of these geochemical affinities coincide with the characteristics of the younger (supposedly slab breakoff-related) magmas of the Roman Magmatic Province (see below).

[25] The majority of the Tuscan magmas are strongly evolved, and are largely derived from melting of the Tuscan basement [*Poli*, 2004]. Mantle-derived mafic magmas contain subduction components but there are rocks with higher La/Nb and Ca/Al (e.g., shoshonites versus older calc-alkaline rocks at Capraia). Higher Ca/Al and lower Sr isotope ratios mean higher proportions of asthenospheric component than metasomatized lithospheric mantle, which agrees with the presence of deep faults allowing deep mantle to contribute to magmatism. We therefore interpret such magmatism as slab tear-related magmatism (Figure 9) involving deeper asthenospheric mantle-derived melts, which either rose to the surface and produced relatively primitive magmas (shoshonites of Capraia and Campiglia dyke) or provided additional heat for the melting of the lithospheric mantle and continental crust (Tolfa-Manziana-Cerite, Roccastrada, San Vincenzo, and southern Tuscany granitoids). We emphasize, however, that the more evolved felsic magmas do not enable us to constrain the geochemical characteristics of the mantle. Their association with possible tear faulting is therefore predominantly based on their temporal and spatial distribution.

[26] In the central Apennines, slab breakoff following tearing coincided with the generation of magmas in the Roman Magmatic Province (Vulsini, Vico-Sabatini and Alban Hills, Figure 9). These relatively late (<1 Ma) volcanic complexes are characterized by potassic and high-potassic magmas, developed in a zone of NW-SE trending normal faults [*Peccerillo*, 1990, 2005]. These magmatic centers are situated northwest of the central Apennine asthenospheric window (Figure 6e), and could have possibly been triggered by the final breakoff of the lithospheric slab. Activity at Mt Ernici and Roccamonfina marks the transition between the slab breakoff magmatism and the tear-related activity of the Pontine Islands (Ponza, Ventotene, and Palmarola) and Campania province (Ischia, Procida, Phlegrean Fields, and Vesuvius).

[27] The two most striking examples of asthenospheric upwelling along slab tear faults are Mt Etna [*Gvirtzman and Nur*, 1999; *Doglioni et al.*, 2001; *Trua et al.*, 2003] and Mt Vulture [*De Astis et al.*, 2006] (Figure 9). These volcanoes are situated on the margin of the foreland and are therefore much less affected by subduction processes. Mt Etna is characterized by a typical Ocean Island Basalt (OIB) composition with some arc signatures in the younger products [*Schiano et al.*, 2001] (Figure 8b). The source of magmatism in Vulture is similar to the Campanian-Pontine volcanoes (Vesuvius, Phlegraean Fields), but its position over the edge of the Adriatic continental lithosphere resulted

in a higher level of intraplate (OIB type) mantle influence [*De Astis et al.*, 2006].

[28] The Aeolian Islands and associated seamounts are typical subduction-related volcanoes, with the oceanic or thinned continental Ionian slab actively subducting beneath their eastern sector. They are characterized by relatively low $^{87}Sr/^{86}Sr$ values (Figure 8b) in the western sector, and represent oceanic arc volcanism. We recognize, however, an enhanced magmatic activity (Vulcano, Lipari and Salina) and an apparent offset along the tear fault that connects the arc with Mt Etna to the southeast (Figure 5). The westernmost island of Alicudi is characterized by rather low La/Nb and $^{87}Sr/^{86}Sr$ values, similar to those of Etna and Ustica, suggesting a stronger asthenospheric influence. Also the Island of Stromboli has relatively low LILE/HFSE, resembling Campanian volcanoes for several incompatible element ratios and radiogenic isotope signatures [*Peccerillo*, 2001]. Its position at the margin of the arc and similar geochemical signatures as the Campanian rocks also support input of OIB-type components for Stromboli. The south Tyrrhenian seamounts and ocean floor with MORB, back-arc, and OIB affinity are also related to the asthenospheric upwelling that accompanied the opening of the Tyrrhenian Sea.

[29] The role of slab tearing seems to be somewhat less significant in controlling the distribution of kamafugitic-melilititic and lamproites magmas in the northern Apennines. Figure 8a shows the geochemical similarity between the kamafugitic-melilititic magmas and the slab breakoff magmas of the Roman Magmatic Province. This suggests a common metasomatized lithospheric mantle origin [*Peccerillo*, 2005]. However, their spatial distribution was predominantly controlled by crustal structures associated with a rift-related postcollisional environment [*Peccerillo*, 2005; *Peccerillo and Martinotti*, 2006]. Similarly, the ascent of lamproitic magmas, originated from a metasomatized lithospheric mantle [*Peccerillo and Martinotti*, 2006] with a strong crustal signature (Figure 8a), was controlled by extensional crustal structures.

6. Discussion and Conclusions

[30] In this study, we combined seismic tomography data and kinematic reconstructions to obtain a deeper insight into the complex geodynamics of Italian magmatism. On the basis of our model, tear faulting and slab breakoff played a fundamental role in controlling the temporal and spatial distribution of young (< 10 Ma) magmatism in this region. We recognize that magmatic activity induced by tear faulting was a transitional phase between subduction-related arc magmatism and postcollisional magmas related to slab breakoff. This tectono-magmatic evolution marks the destruction of subduction zones, indicating the fate of subducting slabs following continental collision.

[31] The role of components with low LILE/HFSE in the origin of Italian magmatism has been long recognized and has been attributed to various processes. Some authors believe this was a resident end-member in the premetasomatic uppermost mantle [*Ellam et al.*, 1989], while others suggest an origin from a deep-mantle plume [*Gasperini et al.*, 2002]. A mantle inflow from the foreland region has also been suggested [*Trua et al.*, 2003; *Peccerillo*, 2001, 2005; *De Astis et al.*, 2006]. However, low LILE/HFSE magmas are widespread along the Italian orogenic volcanic belt and mostly concentrated in zones of lithospheric vertical discontinuities, as shown earlier. Therefore, our hypothesis of deep asthenospheric origin of low LILE/HFSE magmas and their rise along slab-tearing discontinuities represents a much more unifying and simple mechanism in comparison with previous suggestions.

[32] The magmatic signature associated with tear faulting is important because it can considerably enhance our ability to reconstruct modern and ancient convergent plate boundaries. Tear faults, unlike strike-slip faults that are associated with oblique collision or indentation [*Woodcock and Daly*, 1986], are characterized by magmatic activity induced by upwelling of asthenospheric material. Their geometry is attained by tearing and segmentation of lithospheric slabs during subduction rollback. In most retreating plate boundaries, this process is inevitable. This is because the subducting lithosphere is not uniform but typically consists of numerous seamounts, oceanic plateaus, aseismic ridges and continental fragments [*Ben-Avraham et al.*, 1981; *Cloos*, 1993]. Since these lithospheric anomalies are relatively buoyant, their arrival at the subduction zone is likely to impede subduction rollback, thus dividing the subduction zone into segments of different rollback velocities. Tomographic evidence from the northwestern Pacific suggests that slab tearing occurred at areas where seamount chains have been subducting [*van der Hilst and Seno*, 1993; *Levin et al.*, 2002; *Miller et al.*, 2004, 2005, 2006]. Many of the Pacific examples involved subduction of relatively narrow aseismic ridges, which only locally reduced rollback velocities and were therefore responsible for the development of a cuspate shape. Other examples, such as the stepping of the Palau Yap trench in the area where the Caroline Ridge arrived at the subduction zone, could possibly represent slab tear faults. It is emphasized, however, that the response to the arrival of seamounts, oceanic plateaus or island arcs at the subduction zone depends of their relative contribution to the gross lithospheric buoyancy [*Cloos*, 1993]. Therefore, the dynamic effect associated with the arrival of continental Adria at the subduction zone would be more pronounced than the effect associated with aseismic ridge subduction.

[33] It is therefore likely that lithospheric-scale orogen-perpendicular structures exist in other modern and ancient convergent plate boundaries. Evidence for the existence of such structures has been reported, for example, from the New Guinea Fold Belt, where orogen-perpendicular transfer faults were found to be associated with non-subduction-related magmatism and Cu-Au mineralization [*Hill et al.*, 2002]. In addition, there is increasing geochemical evidence for magmatism in orogenic belts that is not directly related to subduction processes, and is attributed instead to the process of slab tearing or slab breakoff [e.g., *Caprarelli and Leitch*, 2001; *Seghedi et al.*, 2004; *Portnyagin et al.*, 2005; *Hoernle et al.*, 2006]. Such information could possibly be

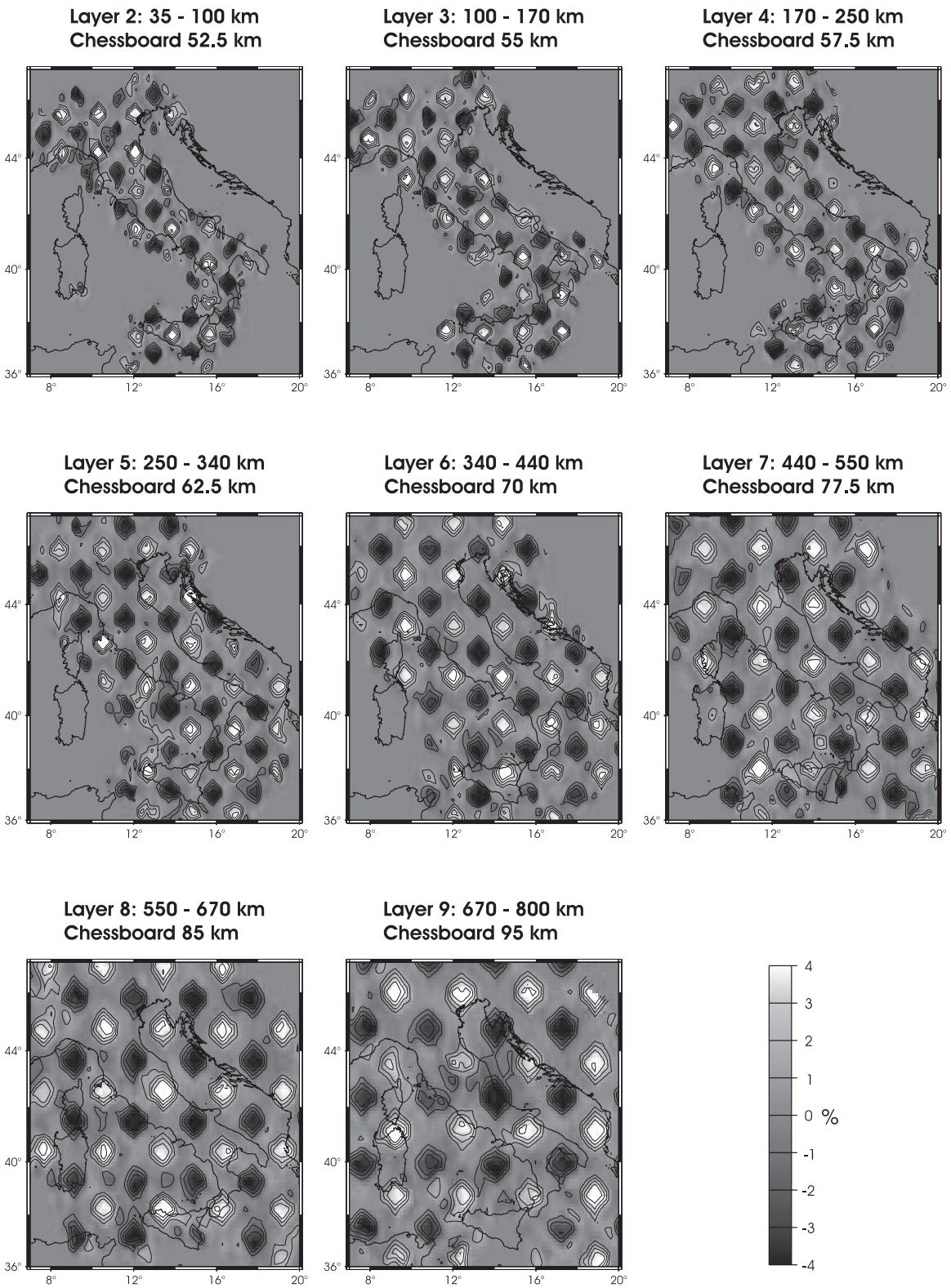

Figure A1. Chessboard recovery test in map views for the layers of the tomographic model by *Lucente et al.* [1999]. Input heterogeneities of opposite sign (±4%) are alternately superimposed on the ambient velocity in each layer. The input anomalies have wavelength equal to the block dimensions in each layer and are separated by unperturbed blocks. Gaussian random noise is added to the data before inversion (standard deviation 0.5 s) to mimic observational errors in the real data. The output model is given in gray shades.

correlated with major crustal lineaments, thus providing a novel approach for reconstructing the geodynamics of ancient plate boundaries.

Appendix A: Sensitivity Analyses

[34] In this section we present a set of sensitivity tests [e.g., *van der Hilst et al.*, 1993; *Piromallo and Morelli*, 2003; *Huang and Zhao*, 2006] applied to the tomographic model of *Lucente et al.* [1999] (hereinafter L99). The purpose of these analyses is to address the resolution of the inversion scheme in terms of its ability to retrieve a known input model, given the same ray coverage used for the real data inversion. For a comprehensive evaluation of the resolution power it is necessary to refer to L99, where the method-data apparatus is described in detail. The sensitivity analyses allow a comprehensive, relatively rapid, visual inspection of the model's spatial resolution. However, being a limited representation of the resolution matrix (R), they can only provide a qualitative estimate of the resolution. Therefore, results of the following synthetic tests need to be read together with the analysis of the resolution matrix (R), which represents a higher-rank diagnostic factor for assessing the reliability of the estimated model in an inversion procedure. The resolution matrix (R), (both diagonal and off-diagonal elements) is analyzed and discussed by L99.

[35] In order to assess the resolution power of the data-method ensemble for structures of different wavelengths, we performed various synthetic tests, modifying size and distribution of the synthetic anomalies in the model. Travel times in the synthetic models are computed by forward calculation with the same theoretical apparatus used for the actual inversion by L99 (i.e., the ACH inversion technique [*Aki et al.*, 1977]). Using this approach, we maintain some of the implicit ACH limitations, such as the use of 1-D ray tracing. The actual inversion by L99 consists of ~6000 accurately repicked arrival times, for which the scatter of the relative residuals population is estimated to be contained within 0.3 s (see L99). Travel times through the synthetic models are reinverted adding Gaussian random noise with 0.5 s standard deviation. This more conservative value for the random noise added to the synthetic data ensures that the actual noise affecting the inverted data is not underestimated. Input parameters for the synthetic models (i.e., block dimensions, minimum number of rays for each block, damping factor, etc.) are same to those in the actual data and are reported in L99.A detailed representation of the sensitivity analyses is provided in Figure A1 and the auxiliary material Figures S1–S4.

[36] Figure A1 shows results of a chessboard test, where the input heterogeneities of alternating sign (±4%) and wavelength equal to the block dimensions in each layer are superimposed by the ambient mantle velocity at that the layer's depth. Block dimensions increase from 52.5 to 95 km with increasing layer depth and are separated by unperturbed blocks. We observe that horizontal smearing of anomalies mainly occurs in the peripheral regions of the model, where ray sampling is poor and/or strongly anisotropic. In the internal parts of the model, where structural elements discussed in this paper are located, heterogeneities are satisfactorily retrieved down to wavelengths comparable to the block dimension in each layer, and almost in the whole depth range. Only in the lowermost layer (670–800 km depth), we observe smearing effects in the central part of the model and an amplitude decays of anomalies. In this depth range, the central part of the model is characterized by relatively lower values (<0.6) of the resolution matrix diagonal elements (see L99 and auxiliary material Figures S1–S3).

[37] **Acknowledgments.** This research was supported by a University of Queensland Early Career Researcher grant to G. R. We wish to thank R. Govers, K. Collerson, P. Vasconcelos, and T. Uysal for providing critical comments on earlier versions of this manuscript. The paper benefited from critical reviews by A. Malinverno and an anonymous reviewer.

References

Aki, K., A. Christofferson, and E. Husebye (1977), Determination of three-dimensional seismic structure of lithosphere, *J. Geophys. Res.*, *82*, 277–296, doi:10.1029/JB082i002p00277.

Ben-Avraham, Z., A. Nur, D. Jones, and A. Cox (1981), Continental accretion: From oceanic plateaus to allochthonous terranes, *Science*, *213*, 47–54, doi:10.1126/science.213.4503.47.

Billi, A., G. Barberi, C. Faccenna, G. Neri, F. Pepe, and A. Sulli (2006), Tectonics and seismicity of the Tindari Fault System, southern Italy: Crustal deformations at the transition between ongoing contractional and extensional domains located above the edge of a subducting slab, *Tectonics*, *25*, TC2006, doi:10.1029/2004TC001763.

Bird, P. (1978), Initiation of intracontinental subduction in the Himalaya, *J. Geophys. Res.*, *83*, 4975–4987, doi:10.1029/JB083iB10p04975.

Bird, P. (1979), Continental delamination and the Colorado Plateau, *J. Geophys. Res.*, *84*, 7561–7571.

Bruno, P. P., V. Di Fiore, and G. Ventura (2000), Seismic study of the '41st parallel' fault system offshore the Campanian-Latial continental margin, Italy, *Tectonophysics*, *324*, 37–55, doi:10.1016/S0040-1951(00)00114-1.

Cadoux, A., D. L. Pinti, C. Aznar, S. Chiesa, and P.-Y. Gillot (2005), New chronological and geochemical constraints on the genesis and geological evolution of Ponza and Palmarola Volcanic Islands (Tyrrhenian Sea, Italy), *Lithos*, *81*, 121–151, doi:10.1016/j.lithos.2004.09.020.

Caprarelli, G., and E. C. Leitch (2001), Geochemical evidence from Lower Permian volcanic rocks of northeast New South Wales for asthenospheric upwelling following slab breakoff, *Aust. J. Earth Sci.*, *48*, 151–166, doi:10.1046/j.1440-0952.2001.00850.x.

Carminati, E., M. J. R. Wortel, W. Spakman, and R. Sabadini (1998), The role of slab detachment processes in the opening of the western-central Mediterranean basins: Some geological and geophysical evidence, *Earth Planet. Sci. Lett.*, *160*, 651–665, doi:10.1016/S0012-821X(98)00118-6.

Castello, B., M. Moro, C. Chiarabba, M. Di Bona, F. Doumaz, G. Selvaggi, and A. Amato (2004), Seismicity map of Italy, map, Inst. Naz. di Geofis. e Vulcanol, Rome.

Chatelain, J.-L., P. Molnar, R. Prevot, and B. Isacks (1992), Detachment of part of the downgoing slab and uplift of the New Hebrides (Vanuatu) islands, *Geophys. J. Int.*, *19*, 1507–1510.

Civetta, L., G. Orsi, P. Scandone, and R. Pece (1978), Eastwards migration of the Tuscan anatectic magmatism due to anticlockwise rotation of the Apennines, *Nature*, *276*, 604–606, doi:10.1038/276604a0.

Cloos, M. (1993), Lithospheric buoyancy and collisional orogenesis: subduction of oceanic plateaus, continental margins, island arcs, spreading ridges, and seamounts, *Geol. Soc. Am. Bull.*, *105*, 715–737, doi:10.1130/0016-7606(1993)105<0715:LBACOS>2.3.CO;2.

Cloos, M., B. Sapiie, A. Quarles van Ufford, R. J. Weiland, P. Q. Warren, and T. P. McMahon (2005), Collisional delamination in New Guinea: The geotectonics of subducting slab breakoff, *Spec. Pap. Geol. Soc. Am.*, *400*, 48 pp.

Davies, J. H., and F. von Blanckenburg (1995), Slab breakoff: A model of lithosphere detachment and its test in the magmatism and deformation of collisional orogens, *Earth Planet. Sci. Lett.*, *129*, 85–102, doi:10.1016/0012-821X(94)00237-S.

De Astis, G., P. D. Kempton, and A. Peccerillo (2006), Trace element and isotopic variations from Mt. Vulture to Campanian volcanoes: Constraints for slab detachment and mantle inflow beneath southern Italy, *Con-*

trib. Mineral. Petrol., *151*, 331–351, doi:10.1007/s00410-006-0062-y.

Decandia, F. A., A. Lazzarotto, and D. Liotta (2001), Structural features of southern Tuscany, Italy, *Ofioliti*, *26*, 287–300.

Dewey, J. F., M. L. Helman, E. Turco, D. H. W. Hutton, and S. D. Knott (1989), Kinematics of the western Mediterranean, in *Alpine Tectonics*, edited by M. P. Coward, D. Dietrich, and R. G. Park, *Spec. Publ. Geol. Soc.*, *45*, 265–283.

Di Luccio, F., A. Piscini, N. A. Pino, and G. Ventura (2005), Reactivation of deep faults beneath Southern Apennines: Evidence from the 1990–1991 Potenza seismic sequences, *Terra Nova*, *17*, 586–590, doi:10.1111/j.1365-3121.2005.00653.x.

Doglioni, C., F. Mongelli, and P. Pieri (1994), The Puglia uplift (SE Italy): An anomaly in the foreland of the Apenninic subduction due to buckling of a thick continental lithosphere, *Tectonics*, *13*, 1309–1321, doi:10.1029/94TC01501.

Doglioni, C., P. Harabaglia, S. Merlini, F. Mongelli, A. Peccerillo, and C. Piromallo (1999), Orogens and slabs vs. their direction of subduction, *Earth Sci. Rev.*, *45*, 167–208, doi:10.1016/S0012-8252(98)00045-2.

Doglioni, C., F. Innocenti, and G. Mariotti (2001), Why Mt. Etna?, *Terra Nova*, *13*, 25–31, doi:10.1046/j.1365-3121.2001.00301.x.

Ellam, R. M., M. A. Menzies, C. J. Hawkesworth, and N. W. Rogers (1989), The volcanism of southern Italy: Role of subduction and the relationship between potassic and sodic alkaline magmatism, *J. Geophys. Res.*, *94*, 4589–4601, doi:10.1029/JB094iB04p04589.

Faccenna, C., T. W. Becker, F. P. Lucente, L. Jolivet, and F. Rosseti (2001), History of subduction and back-arc extension in the Central Mediterranean, *Geophys. J. Int.*, *145*, 809–820, doi:10.1046/j.0956-540x.2001.01435.x.

Faccenna, C., L. Civetta, M. D'Antonio, F. Funiciello, L. Margheriti, and C. Piromallo (2005), Constraints on mantle circulation around the deforming Calabrian slab, *Geophys. Res. Lett.*, *32*, L06311, doi:10.1029/2004GL021874.

Faccenna, C., O. Bellier, J. Martinod, C. Piromallo, and V. Regard (2006), Slab detachment beneath eastern Anatolia: A possible cause for the formation of the North Anatolian fault, *Earth Planet. Sci. Lett.*, *242*, 85–97, doi:10.1016/j.epsl.2005.11.046.

Frezzotti, M. L., G. de Astis, L. Dallai, and C. Ghezzo (2007), Coexisting calc-alkaline and ultrapotassic magmatism at Monti Ernici, Mid Latina Valley (Latium, central Italy), *Eur. J. Mineral.*, *19*, 479–497, doi:10.1127/0935-1221/2007/0019-1754.

Funiciello, F., C. Faccenna, D. Giardini, and K. Regenauer-Lieb (2003), Dynamics of retreating slabs: 2. Insights from three-dimensional laboratory experiments, *J. Geophys. Res.*, *108*(B4), 2207, doi:10.1029/2001JB000896.

Gasperini, D., J. Blichert-Toft, D. Bosch, A. Del Moro, P. Macera, and F. Albarède (2002), Upwelling of deep mantle material through a plate window: Evidence from the geochemistry of Italian basaltic volcanics, *J. Geophys. Res.*, *107*(B12), 2367, doi:10.1029/2001JB000418.

Gerya, T. V., D. A. Yuen, and W. V. Maresch (2004), Thermomechanical modelling of slab detachment, *Earth Planet. Sci. Lett.*, *226*, 101–116, doi:10.1016/j.epsl.2004.07.022.

Goes, S., D. Giardini, S. Jenny, C. Hollenstein, H. G. Kahle, and A. Geiger (2004), A recent tectonic reorganization in the south-central Mediterranean, *Earth Planet. Sci. Lett.*, *226*, 335–345, doi:10.1016/j.epsl.2004.07.038.

Govers, R., and M. J. R. Wortel (2005), Lithosphere tearing at STEP faults: Response to edges of subduction zones, *Earth Planet. Sci. Lett.*, *236*, 505–523, doi:10.1016/j.epsl.2005.03.022.

Guivel, C., et al. (2006), Miocene to Late Quaternary Patagonian basalts (46–47°S): Geochronometric and geochemical evidence for slab tearing due to active spreading ridge subduction, *J. Volcanol. Geotherm. Res.*, *149*, 346–370, doi:10.1016/j.jvolgeores.2005.09.002.

Gvirtzman, Z., and A. Nur (1999), The formation of Mount Etna as the consequence of slab rollback, *Nature*, *401*, 782–785, doi:10.1038/44555.

Hill, K. C., R. D. Kendrick, P. V. Crowhurst, and P. A. Gow (2002), Copper-gold mineralisation in New Guinea: Tectonics, lineaments, thermochronology and structure, *Aust. J. Earth Sci.*, *49*, 737–752, doi:10.1046/j.1440-0952.2002.00944.x.

Hoernle, K., et al. (2006), Cenozoic intraplate volcanism on New Zealand: Upwelling induced by lithospheric removal, *Earth Planet. Sci. Lett.*, *248*, 335–367, doi:10.1016/j.epsl.2006.06.001.

Hollenstein, C., H. G. Kahle, A. Geiger, S. Jenny, S. Goes, and D. Giardini (2003), New GPS constraints on the Africa-Eurasia plate boundary zone in southern Italy, *Geophys. Res. Lett.*, *30*(18), 1935, doi:10.1029/2003GL017554.

Houseman, G. A., D. P. McKenzie, and P. Molnar (1981), Convective instability of a thickened boundary layer and its relevance for the thermal evolution of continental convergent belts, *J. Geophys. Res.*, *86*, 6115–6132, doi:10.1029/JB086iB07p06115.

Huang, J., and D. Zhao (2006), High-resolution mantle tomography of China and surrounding regions, *J. Geophys. Res.*, *111*, B09305, doi:10.1029/2005JB004066.

Kincaid, C., and R. W. Griffiths (2003), Laboratory models of the thermal evolution of the mantle during rollback subduction, *Nature*, *425*, 58–62, doi:10.1038/nature01923.

Lallemand, S., Y. Font, H. Bijwaard, and H. Kao (2001), New insights on 3-D plates interaction near Taiwan from tomography and tectonic implications, *Tectonophysics*, *335*, 229–253, doi:10.1016/S0040-1951(01)00071-3.

Lentini, F., S. Carbone, and S. Catalano (1994), Main structural domains of the Central Mediterranean region and their Neogene tectonic evolution, *Boll. Geofis. Teor. Appl.*, *36*, 103–125.

Levin, V., N. Shapiro, J. Park, and M. Ritzwoller (2002), Seismic evidence for catastrophic slab loss beneath Kamchatka, *Nature*, *418*, 763–767, doi:10.1038/nature00973.

Lucente, F. P., and F. Speranza (2001), Belt bending driven by lateral bending of subducting lithospheric slab: Geophysical evidences from the Northern Apennines (Italy), *Tectonophysics*, *337*, 53–64, doi:10.1016/S0040-1951(00)00286-9.

Lucente, F. P., C. Chiarabba, G. B. Cimini, and D. Giardini (1999), Tomographic constraints on the geodynamic evolution of the Italian region, *J. Geophys. Res.*, *104*, 20,307–20,327, doi:10.1029/1999JB900147.

Malinverno, A., and W. B. F. Ryan (1986), Extension on the Tyrrhenian Sea and shortening in the Apennines as result of arc migration driven by sinking of the lithosphere, *Tectonics*, *5*, 227–245, doi:10.1029/TC005i002p00227.

Marani, M. P., and T. Trua (2002), Thermal constriction and slab tearing at the origin of a superinflated spreading ridge: Marsili volcano (Tyrrhenian Sea), *J. Geophys. Res.*, *107*(B9), 2188, doi:10.1029/2001JB000285.

Martin, A. K. (2006), Oppositely directed pairs of propagating rifts in back-arc basins: Double saloon door seafloor spreading during subduction rollback, *Tectonics*, *25*, TC3008, doi:10.1029/2005TC001885.

Mattei, M., V. Petrocelli, D. Lacava, and M. Schiattarella (2004), Geodynamic implications of Pleistocene ultrarapid vertical-axis rotations in the Southern Apennines, Italy, *Geology*, *32*, 789–792, doi:10.1130/G20552.1.

Maury, R. C., et al. (2000), Post-collisional Neogene magmatism of the Mediterranean Maghreb margin: A consequence of slab breakoff, *C. R. Acad. Sci., Ser. IIa*, *331*, 159–173.

Miller, M. S., B. L. N. Kennett, and G. S. Lister (2004), Imaging changes in morphology, geometry, and physical properties of the subducting Pacific plate along the Izu-Bonin-Mariana arc, *Earth Planet. Sci. Lett.*, *224*, 363–370, doi:10.1016/j.epsl.2004.05.018.

Miller, M. S., A. Gorbatov, and B. L. N. Kennett (2005), Heterogeneity within the subducting Pacific slab beneath the Izu-Bonin-Mariana arc: Evidence from tomography using 3D ray tracing inversion techniques, *Earth Planet. Sci. Lett.*, *235*, 331–342, doi:10.1016/j.epsl.2005.04.007.

Miller, M. S., A. Gorbatov, and B. L. N. Kennett (2006), Three-dimensional visualization of a near-vertical slab tear beneath the southern Mariana arc, *Geochem. Geophys. Geosyst.*, *7*, Q06012, doi:10.1029/2005GC001110.

Panza, G. F., A. Peccerillo, A. Aoudia, and B. Farina (2007), Geophysical and petrological modelling of the structure and composition of the crust and upper mantle in complex geodynamic settings: The Tyrrhenian Sea and surroundings, *Earth Sci. Rev.*, *80*, 1–46, doi:10.1016/j.earscirev.2006.08.004.

Patacca, E., and P. Scandone (1989), Post-Tortonian mountain building in the Apennines. The role of the passive sinking of a relic lithospheric slab, in *The Lithosphere in Italy*, edited by A. Boriani, et al., pp. 157–176, Ital. Natl. Comm. for the Int. Lithosphere Program, Rome.

Peccerillo, A. (1990), On the origin of the Italian potassic magmas—Comments, *Chem. Geol.*, *85*, 183–191, doi:10.1016/0009-2541(90)90130-Y.

Peccerillo, A. (2001), Geochemical similarities between the Vesuvius, Phlegraean Fields and Stromboli Volcanoes: Petrogenetic, geodynamic and volcanological implications, *Mineral. Petrol.*, *73*, 93–105, doi:10.1007/s007100170012.

Peccerillo, A. (2005), *Plio-Quaternary Volcanism in Italy*, 365 pp., Springer, Berlin.

Peccerillo, A., and G. Martinotti (2006), The Western Mediterranean lamproitic magmatism: Origin and geodynamic significance, *Terra Nova*, *18*, 109–117, doi:10.1111/j.1365-3121.2006.00670.x.

Peccerillo, A., and G. F. Panza (1999), Upper mantle domains beneath central-southern Italy: Petrological, geochemical and geophysical constraints, *Pure Appl. Geophys.*, *156*, 421–443, doi:10.1007/s000240050306.

Piromallo, C., and A. Morelli (2003), *P* wave tomography of the mantle under the Alpine-Mediterranean area, *J. Geophys. Res.*, *108*(B2), 2065, doi:10.1029/2002JB001757.

Platt, J. P., and P. C. England (1994), Convective removal of lithosphere beneath mountain belts: Thermal and mechanical consequences, *Am. J. Sci.*, *294*, 307–336.

Poli, G. (2004), Genesis and evolution of miocene-quaternary intermediate-acid rocks from the Tuscan magmatic province, *Period. Mineral.*, *73*, 187–214.

Portnyagin, M., K. Hoernle, G. Avdeiko, F. Hauff, R. Werner, I. Bindeman, V. Uspensky, and D. Garbe-Schönberg (2005), Transition from arc to oceanic magmatism at the Kamchatka-Aleutian junction, *Geology*, *33*, 25–28, doi:10.1130/G20853.1.

Renda, P., E. Tavarnelli, M. Tramutoli, and E. Gueguen (2000), Neogene deformation of northern Sicily, and their implications for the geodynamics of the southern Tyrrhenian Sea margin, *Mem. Soc. Geol. It.*, *55*, 53–59.

Rosenbaum, G., and G. S. Lister (2004), Neogene and Quaternary rollback evolution of the Tyrrhenian Sea, the Apennines and the Sicilian Maghrebides, *Tectonics*, *23*, TC1013, doi:10.1029/2003TC001518.

Rosenbaum, G., G. S. Lister, and C. Duboz (2002), Relative motions of Africa, Iberia and Europe during Alpine orogeny, *Tectonophysics*, *359*, 117–129, doi:10.1016/S0040-1951(02)00442-0.

Royden, L., E. Patacca, and P. Scandone (1987), Segmentation and configuration of subducted lithosphere in Italy: An important control on thrust-belt and foredeep-basin evolution, *Geology*, *15*, 714–717, doi:10.1130/0091-7613(1987)15<714:SACOSL>2.0.CO;2.

Sacks, P. E., and D. T. Secor (1990), Delamination in collisional orogens, *Geology*, *18*, 999–1002, doi:10.1130/0091-7613(1990)018<0999:DICO>2.3.CO;2.

Sartori, R. (1986), Notes on the geology of the acoustic basement in the Tyrrhenian Sea, *Mem. Soc. Geol. It.*, *36*, 99–108.

Sartori, R. (1990), The main results of ODP Leg 107 in the frame of Neogene to Recent geology of Perityrrhenian areas, *Proc. Ocean Drill. Program Sci. Results*, *107*, 715–730.

Sartori, M. (2005), Bedrock geology of the Tyrrhenian Sea: Insight on Alpine paleogeography and magmatic evolution of the basin, in *CROP PROJECT: Deep Seismic Exploration of the Central Mediterranean and Italy*, edited by I. R. Finetti, pp. 69–80, Elsevier, Amsterdam.

Schellart, W. P. (2004), Kinematics of subduction and subduction-induced flow in the upper mantle, *J. Geophys. Res.*, *109*, B07401, doi:10.1029/2004JB002970.

Schellart, W. P., G. S. Lister, and M. W. Jessell (2002), Analogue modeling of arc and backarc deformation in the New Hebrides Arc and North Fiji Basin, *Geology*, *30*, 311–314, doi:10.1130/0091-7613(2002)030<0311:AMOAAB>2.0.CO;2.

Schellart, W. P., J. Freeman, D. R. Stegman, L. Moresi, and D. May (2007), Evolution and diversity of subduction zones controlled by slab width, *Nature*, *446*, 308–311, doi:10.1038/nature05615.

Schiano, P., R. Clocchiatti, L. Ottolini, and T. Busa (2001), Transition of Mount Etna lavas from a mantle-plume to an island-arc magmatic source, *Nature*, *412*, 900–904, doi:10.1038/35091056.

Scrocca, D. (2006), Thrust front segmentation induced by differential slab retreat in the Apennines (Italy), *Terra Nova*, *18*, 154–161, doi:10.1111/j.1365-3121.2006.00675.x.

Seghedi, I., et al. (2004), Neogene-Quaternary magmatism and geodynamics in the Carpathian-Pannonian region: A synthesis, *Lithos*, *72*, 117–146, doi:10.1016/j.lithos.2003.08.006.

Spadini, G., and F.-C. Wezel (1994), Structural evolution of the "41st parallel zone": Tyrrhenian Sea, *Terra Nova*, *6*, 552–562, doi:10.1111/j.1365-3121.1994.tb00522.x.

Speranza, F., R. Maniscalco, M. Mattei, D. Stefano, and R. W. H. Butler (1999), Timing and magnitude of rotations in the frontal thrust systems of southwestern Sicily, *Tectonics*, *18*, 1178–1197, doi:10.1029/1999TC900029.

Trua, T., G. Serri, and M. P. Marani (2003), Lateral flow of African mantle below the nearby Tyrrhenian plate: Geochemical evidence, *Terra Nova*, *15*, 433–440, doi:10.1046/j.1365-3121.2003.00509.x.

van der Hilst, R., and T. Seno (1993), Effects of relative plate motion on the deep structure and penetration depth of slabs below the Izu-Bonin and Mariana island arcs, *Earth Planet. Sci. Lett.*, *120*, 395–407, doi:10.1016/0012-821X(93)90253-6.

van der Hilst, R. D., E. R. Engdahl, and W. Spakman (1993), Tomographic inversion of P and pP data for aspherical mantle structure below the northwest Pacific region, *Geophys. J. Int.*, *115*, 264–302, doi:10.1111/j.1365-246X.1993.tb05603.x.

van der Meulen, M. J., J. E. Meulenkamp, and M. J. R. Wortel (1998), Lateral shifts of Apennnic foredeep depocentres reflecting detachment of subducted lithosphere, *Earth Planet. Sci. Lett.*, *154*, 203–219, doi:10.1016/S0012-821X(97)00166-0.

van der Meulen, M. J., S. J. H. Buiter, J. E. Meulenkamp, and M. J. R. Wortel (2000), An early Pliocene uplift of the central Apenninic foredeep and its geodynamic significance, *Tectonics*, *19*, 300–313, doi:10.1029/1999TC900064.

Van Dijk, J. P., and P. J. J. Scheepers (1995), Neotectonic rotations in the Calabrian Arc: Implications for a Pliocene-Recent geodynamic scenario for the central Mediterranean, *Earth Sci. Rev.*, *39*, 207–246, doi:10.1016/0012-8252(95)00009-7.

von Blanckenburg, F., and J. H. Davies (1995), Slab breakoff: A model for syncollisional magmatism and tectonics in the Alps, *Tectonics*, *14*, 120–131, doi:10.1029/94TC02051.

Woodcock, N. H., and M. C. Daly (1986), The role of strike-slip fault systems at plate boundaries, *Philos. Trans. R. Soc.*, *317*, 13–29, doi:10.1098/rsta.1986.0021.

Wortel, M. J. R., and W. Spakman (2000), Subduction and slab detachment in the Mediterranean-Carpathian region, *Science*, *290*, 1910–1917, doi:10.1126/science.290.5498.1910.

M. Gasparon and G. Rosenbaum, School of Physical Sciences, University of Queensland, Brisbane, Queensland 4072, Australia. (g.rosenbaum@uq.edu.au)

F. P. Lucente, Istituto Nazionale di Geofisica e Vulcanologia, CNT, Rome I-00143, Italy.

M. S. Miller, Department of Earth Science, Rice University, Houston, TX 77251, USA.

A. Peccerillo, Dipartimento di Scienze della Terra, Università degli Studi di Perugia, Perugia I-06100, Italy.